

Learning for Feasible Region on Coal Mine Virtual Power Plants with Imperfect Information

Hongxu Huang *Member, IEEE*, Ruike Lyu, *Graduate Student Member, IEEE*, Cheng Feng, *Member, IEEE*, Haiwang Zhong *Senior Member, IEEE*, H. B. Gooi *Life Fellow, IEEE*, Bo Li *Member, IEEE*, and Rui Liang *Senior Member, IEEE*

Abstract—The feasible region assessment (FRA) in industrial virtual power plants (VPPs) is driven by the need to activate large-scale latent industrial loads for demand response, making it essential to aggregate these flexible resources for peak regulation. However, the large number of devices and the need for privacy preservation in coal mines pose challenges to accurately aggregating these resources into a cohesive coal mine VPP. In this paper, we propose an efficient and reliable data-driven approach for FRA in the coal mine VPP that can manage incomplete information. Our data-driven FRA algorithm approximates equipment and FRA parameters based on historical energy dispatch data, effectively addressing the challenges of imperfect information. Simulation results illustrate that our method approximates the accurate feasible operational boundaries under dynamic and imperfect information conditions.

Index Terms—Feasible region assessment, data-driven, inverse optimization, aggregation.

I. INTRODUCTION

THE evolution of energy markets has highlighted the potential of Virtual Power Plants (VPPs) for flexible energy management and trading. Unlike distributed energy resources, industrial sectors with huge regular power demands present significant opportunities for large-scale VPP aggregation. As a major energy-intensive industry in China, the coal mines depend heavily on electricity for their production processes, contributing to an annual power demand of 95.1 billion kWh in 2022 [1]. Given this insight, it is essential to activate the dormant flexibility resources within coal mine industrial energy systems (CMIESs).

Under this circumstance, for VPPs to effectively participate in energy markets, the accurate model of industrial energy system is crucial to describe the both energy consumption behaviors and the flexibility of diverse industrial energy systems. Considerable strides have been achieved in industrial energy system modeling. To name a few, Ref. [2] focused on linearizing the complex nonlinear non-convex industrial demand response model for VPP aggregation as a virtual battery model [3]. In [4], a multi-energy industrial park model is proposed to participate in day-ahead energy and reserve markets via VPP aggregation, ensuring all possible deployment requests can be realized. To center on coal mine industries, the associated energy recovery in coal mines are considered in [5] to improve operational economic benefits. Further considering the flexibility in coal transportation, the integration of belt conveyors (BCs) and coal silos for demand response (DR) are modeled in [6] under the energy-transportation coordinated operation framework. Apart from the economic cost, a multi-objective

model of CMIESs dispatching are solved with multitask multi-objective algorithm [7]. For participate in energy trading, Ref. [8] proposed a CMIES model for participating in the integrated energy and carbon trading market, while coal mines are treated as individual entities rather than as an aggregated VPP. However, these mentioned models are designed for coal mine energy dispatching, remaining a notable gap in aggregating the flexibility of CMIESs.

Flexibility aggregation has become a widely researched topic in the field of VPPs. To effectively participate in the energy market, a VPP needs to estimate a feasible region that defines the boundaries within which these aggregated resources can be managed reliably and efficiently. Various approaches are proposed to manage the feasible region assessment (FRA), such as convex hull outer approximation [9] and the Minkowski sum based estimation method [10]. Although these method are effective in FRA problems, they still rely on perfect information of all participants in the VPP aggregation, which neglects the fact that usually all the participants are not willing to share their privacy information. To tackle the imperfect information in FRA, a privacy-preserving based FRA method is proposed in [11] for peer-to-peer energy trading under uncertain renewable energy generation, while it still relies on the probabilistic density function which is hard to get via the model-driven approaches. However, these methods face significant limitations when applied to the CMIESs due to the issue of imperfect information. In CMIES, the vast number of devices and complex interactions between energy units make it difficult to obtain accurate and complete parameter on all CMIESs. The imperfect information of CMIESs makes it exceptionally challenging to aggregate coal mines into a cohesive VPP capable of reliably participating in energy markets. Thus, how to get the accurate feasible region for CMIESs aggregation is still a remaining challenge.

In order to overcome the imperfect information in FRA problems, data-driven based method has gained as a promising approach to estimate feasible region of complex systems like the CMIES. By utilizing the historical optimal dispatching data, the inverse optimization method [12] is developed to infer underlying parameters and constraints that define optimal operational states, allowing for more accurate and adaptive modeling. Ref. [13] leveraged the structure of virtual battery model and proposed Newtown's method based inverse optimization algorithm for FRA. In [14], the data-driven inverse optimization is also developed to solve simplified virtual battery based VPP aggregation among diverse EVs. Although data-driven inverse optimization has made progress, existing

methods struggle with the unique complexities of CMIESs, such as the complex model of belt conveyors, raw coal mining and transportation networks and processes coordination. These systems require real-time, efficient computation under dynamic conditions, which conventional methods still face challenges in computation efficiency and accuracy. Thus, further advancements are needed to adapt these approaches for the specific demands of large-scale CMIESs.

To address the research gaps identified above, this paper proposes the learning-based FRA method for VPP aggregating the CMIESs with imperfect information. The main contributions of this work are summarized as:

- 1) To reduce the computational burden of FRA, an inverse optimization model is developed based on an energy-transportation coordinated CMIES model, revealing the operational boundary without solving the NP-hard Minkowski sum problem.
- 2) A data-driven FRA method is proposed for CMIES aggregation, addressing imperfect information from unknown parameters and data privacy in coal mines.

The remainder of the paper is organized as follows. Section II briefly introduces the coal mine VPP FRA problem. Section III formulates the inverse optimization model of coal mine VPP aggregation with the energy-transportation coordinated CMIES model. Section IV proposes the learning-based FRA method. Case studies are given in Section V with performance analysis. In the end, Section VI concludes this paper.

II. PROBLEM DESCRIPTION

A. Coal Mine VPP FRA

We consider a typical scenario where the coal mine VPP aggregates several CMIESs operate in the distribution network, equipped with essential devices such as generation units, belt conveyors, and energy storage systems. This setup enables the CMIES to offer flexibility by managing its energy resources dynamically. Such flexibility is crucial for helping the distribution network integrate renewable energy and perform peak shaving and valley filling. To quantify this coal mine VPP FRA, we define it rigorously as follows.

Definition 1. *The feasible region of the coal mine VPP is a sub-space of the energy dispatching variables as the range of its power exchange with DSO and belt-conveyors load peak-valley regulation, noted as Ω_V .*

$$\Omega_V := \{(p_{BC,|I|}^{[T]}, p_g^{[T]}) | \text{s.t. } h(p_{BC,|I|}^{[T]}, p_g^{[T]}, x_{|I|}^{[T]}, \Xi_{|I|})=0, \\ g(p_{BC,|I|}^{[T]}, p_g^{[T]}, x_{|I|}^{[T]}, \Xi_{|I|}) \leq 0\} \quad (1)$$

where $p_{BC,|I|}^{[T]}$ denotes the total power consumption of BCs coal mine indexed by $i \in \mathcal{I}^{|I|}$ at all time intervals $t \in \mathcal{T}^{[T]}$. $p_g^{[T]}$ is the total power exchange of the coal mine VPP with the DSO. $x_{|I|}^{[T]}$ and $\Xi_{|I|}$ are the other decision variables and parameters in coal mine optimal energy dispatching.

However, as pointed out, the parameters $\Xi_{|I|}$ are usually unknown to the aggregator. Also, the vast number of equipment

in the coal transportation network makes the of $\Xi_{|I|}$ a high-dimension vector. As defined in Eq. (1), the feasible region is a projection of the aggregated power exchange and peak-valley regulation capacity on the original feasible set, which is a NP-hard problem. Alternatively, one effective way is to leverage the historical optimal dispatching data to learn the surrogate feasible region, denoted as.

$$\tilde{\Omega}_V(\tilde{\Xi}_{|I|}) := \{(p_{BC,|I|}^{[T]}, p_g^{[T]}) | \text{s.t. } \tilde{h}(p_{BC,|I|}^{[T]}, p_g^{[T]}, \tilde{x}_{|I|}^{[T]}, \tilde{\Xi}_{|I|})=0, \\ \tilde{g}(p_{BC,|I|}^{[T]}, p_g^{[T]}, \tilde{x}_{|I|}^{[T]}, \tilde{\Xi}_{|I|}) \leq 0\} \quad (2)$$

Therefore, the idea behind the surrogate model in Eq. (2) is to use the approximated $\tilde{\Xi}_{|I|}$ for getting a $\tilde{\Omega}_V$ close to the real feasible region Ω_V without knowing the true value of $\Xi_{|I|}$. To this end, the coal mine VPP FRA can be formulated as.

$$\min_{\tilde{\Xi}_{|I|} \in [\underline{\Xi}_{|I|}, \bar{\Xi}_{|I|}]} \mathcal{L}(\tilde{\Omega}_V(\tilde{\Xi}_{|I|}), \Omega_V) \quad (3) \\ \text{s.t. } h(p_{BC,|I|}^{[T]}, p_g^{[T]}, \tilde{x}_{|I|}^{[T]}, \tilde{\Xi}_{|I|})=0 \\ g(p_{BC,|I|}^{[T]}, p_g^{[T]}, \tilde{x}_{|I|}^{[T]}, \tilde{\Xi}_{|I|}) \leq 0$$

where \mathcal{L} is a loss function to minimize the assessment error between $\tilde{\Omega}_V(\tilde{\Xi}_{|I|})$ and Ω_V . Hence, the feasible region can be approximated by solving the optimization problem Eq. (3) with historical data. The tractability of Eq. (3) relies on the original problem, which will be discussed in the following section.

III. ENERGY-TRANSPORTATION COORDINATED COAL MINE OPTIMAL SCHEDULING

A. CMIES Configuration

The configuration of the CMIES and the coal transportation network (CTN) is illustrated in Fig. 1. This coordinated energy-transportation system includes wind turbines (WTs), photovoltaic systems (PVs), combined heat and power units (CHPs), microturbines (MTs), regenerative thermal oxidizers (RTOs), and water source heat pumps (WSHPs). Energy storage is provided through the pumped-hydro storage (PHS) and thermal storage tanks (TSTs). These components are integrated to supply both electrical and thermal energy. To facilitate demand response in coal transportation, the CTN is equipped with belt conveyors (BCs) at various levels and silos, utilizing electricity from the CMIES to transport raw coal from the coal face to the coal preparation plant (CPP) according to CTN scheduling.

B. Objective Function

The objective function aims to minimize the operational costs of the coal mine, incorporating expenses from energy trading under the time-varying price κ_{Price} , fuel costs for generation, and maintenance expenses.

$$C_{\text{Sys}} = \sum_{t \in \mathcal{T}} \left(\kappa_{\text{Price}} p_{\text{grid}}^t + \kappa_{\text{CG}}^{\text{fu}} p_{\text{CHP}}^t + C_{\text{OM}}^t \right) \quad (4a) \\ C_{\text{OM}}^t = \kappa_{\text{PV}}^{\text{om}} p_{\text{PV}}^t + \kappa_{\text{WT}}^{\text{om}} p_{\text{WT}}^t + \kappa_{\text{GT}}^{\text{om},e} p_{\text{GT}}^{t,e} + \kappa_{\text{CHP}}^{\text{om}} p_{\text{CHP}}^{t,f} \\ \kappa_{\text{RTO}}^{\text{om}} p_{\text{RTO}}^t + \sum_{j \in N_{\text{BC}}} \kappa_{\text{BC}}^{\text{om},h} p_{\text{BC}}^{t,h} + \kappa_{\text{PHS}}^{\text{om},h} (p_{\text{PHS}}^t + p_{\text{PHSD}}^t)$$

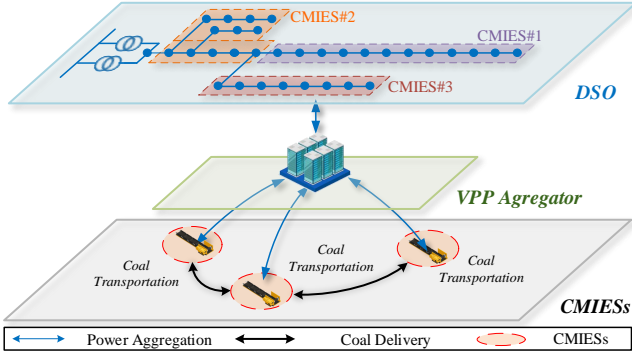


Fig. 1. Coal Mine VPP Aggregation with CMIESs

$$+ \kappa_{TST}^{om,h} (H_{TSC}^t + H_{TSD}^t) + \kappa_{WSHP}^{om,h} p_{WSHP}^t, \quad \forall t \in \mathcal{T} \quad (4b)$$

C. Constraints

1) *Coal Transportation*: The CTN consists of coal faces, BCs, silos, and the CPP, arranged in a radial topology. The CTN can be modeled as a graph $G_{CTN} = \{\sigma_L, T_N\}$, where σ_L and T_N represent the coal transportation links and nodes, respectively. The node set T_N comprises multiple hierarchical nodes, including the coal face supply node T_{CF} , coal silo storage node T_{SS} , transfer node T_{MS} , and the CPP demand node T_{CPP} , expressed as $T_N = \{T_{CF} \cup T_{SS} \cup T_{MS} \cup T_{CPP}\}$. Each BC branch supports coal mass transfer as a flow between nodes at different levels, represented as $\sigma_L = \{\sigma_{CF,SS} \cup \sigma_{SS,MS} \cup \sigma_{MS,CPP}\}$. Coal mass flow proceeds from the coal face to the CPP. The CTN model is formulated as follows.

$$\sigma_{l,m}^t = \frac{Q_{l,m}^t}{3.6 * V_{BC}}, \quad \forall t \in \mathcal{T}, \forall \sigma_{l,m} \in \sigma_{CF,SS} \quad (5a)$$

$$\underline{\sigma}_{l,m}^{ramp} \leq \sigma_{l,m}^t - \sigma_{l,m}^{t-1} \leq \bar{\sigma}_{l,m}^{ramp}, \quad \forall t \in \mathcal{T}, \forall \sigma_{l,m} \in \sigma_{CF,SS} \quad (5b)$$

$$\sum_l \sigma_{l,m}^t \leq \sigma_{m,n}^t \leq \bar{\sigma}_{m,n}, \quad \forall t \in \mathcal{T}, \forall \sigma_{l,m} \in \sigma_{CF,SS}, \quad \forall \sigma_{l,m} \in \sigma_{SS,MS} \quad (5c)$$

$$\sum_t Q_{l,m}^t \leq \sum_t Q_{n,p}^t \leq Q_{L,CPP}, \quad \forall t \in \mathcal{T}, \forall \sigma_{l,m} \in \sigma_{CF,SS}, \quad \forall \sigma_{n,p} \in \sigma_{MS,CPP} \quad (5d)$$

where $Q_{l,m}^t$ and $\sigma_{l,m}^t$ represent the feed rate and coal mass in coal transportation between coal faces and shaft silos respectively. $\underline{\sigma}_{l,m}^{ramp}$ and $\bar{\sigma}_{l,m}^{ramp}$ represent the minimal and maximal ramp limits of coal mass delivery respectively. $\bar{\sigma}_{m,n}$ denotes the maximal limits of coal mass delivered from shaft silos to the main silo. $Q_{L,CPP}$ is the coal mass load in the CPP. Since coal mass flows only in one direction, l, m, n , and p represent the CTN nodes T_{CF}, T_{SS}, T_{MS} and T_{CPP} with the sequence from the coal face to the CPP.

To describe the virtual energy storage characteristic in the CTN, the model of a coal silo is equivalent to the battery model without considering decay. The model is described as:

$$M_{Silo,k}^{t+1} = M_{Silo,k}^t + \sigma_{BC,jk}^t - \sigma_{BC,kj}^t, \quad \forall t \in \mathcal{T}, \forall k \in N_{Silo} \quad (6a)$$

$$\underline{M}_{Silo} \leq M_{Silo,k}^t \leq \bar{M}_{Silo}, \quad \forall t \in \mathcal{T}, \forall k \in N_{Silo} \quad (6b)$$

$$M_{Silo}^1 = M_{Silo}^{st}, \quad M_{Silo}^{24} = M_{Silo}^{end} \quad (6c)$$

2) *Energy Units*: For the electrical and thermal power coupled energy units, the RTO, the CHP, the GT and the WSHP model are formulated as follows.

$$p_X^t = EHR_X * h_X^t, \quad \forall t \in \mathcal{T} \quad (7a)$$

$$\underline{h}_X < h_X^t \leq \bar{h}_X, \quad \forall t \in \mathcal{T} \quad (7b)$$

$$X \in \{RTO, CHP, GT, WSHP\} \quad (7c)$$

where EHR_X is the electricity and heat generation ratio of unit X .

3) *Belt Conveyors*: BCs carry produced raw coal from the work face to the CPP by consuming electricity. The electric power consumption of BCs can be represented using a generalized coal transportation model based on well-known standards or specifications, such as ISO 5048, DIN 22101, JIS B 8805, formulated as follows.

$$p_{BC,j}^t = cof_{BC} \left[\theta_{2,j} V_{BC} + \left(\theta_{4,j} + \frac{V_{BC}}{3.6} \right) Q_{BC,j}^t \right], \quad \forall t \in \mathcal{T}, \forall j \in N_{BC} \quad (8a)$$

4) *Energy Storage Units*: The PHS systems established in abandoned coal mine goaves provide flexible options for storing and releasing electrical energy. Similar to PHS, TSTs are also utilized to mitigate peak thermal loads. The energy storage units are represented by Eqs. (9) and (10).

$$E_{PHS}^{t+1} = \gamma_{PHS} E_{PHS}^t + \eta_{PHS} (p_{PHSC}^t - p_{PHSD}^t), \quad \forall t \in \mathcal{T} \quad (9a)$$

$$E_{PHS}^t \in [\underline{E}_{PHS}, \bar{E}_{PHS}], \quad (9b)$$

$$p_{PHSC}^t \in [\underline{p}_{PHSC}, \bar{p}_{PHSC}], p_{PHSD}^t \in [\underline{p}_{PHSD}, \bar{p}_{PHSD}], \quad (9c)$$

$$E_{PHS}^1 = E_{PHS}^{st}, \quad E_{PHS}^{24} = E_{PHS}^{end} \quad (9d)$$

$$E_{TST}^{t+1} = \gamma_{TST} E_{TST}^t + \eta_{TST} (h_{TSTC}^t - h_{TSTD}^t), \quad \forall t \in \mathcal{T} \quad (10a)$$

$$E_{TST}^t \in [\underline{E}_{TST}, \bar{E}_{TST}], \quad (10b)$$

$$h_{TSTC}^t \in [\underline{h}_{TSTC}, \bar{h}_{TSTC}], h_{TSTD}^t \in [\underline{h}_{TSTD}, \bar{h}_{TSTD}], \quad (10c)$$

$$E_{TST}^1 = E_{TST}^{st}, \quad E_{TST}^{24} = E_{TST}^{end} \quad (10d)$$

5) *Energy Balance*: The electrical and thermal power balance constraints for the coal mines are formulated as follows.

$$\underline{p}_g \leq p_g^t \leq \bar{p}_g, \quad \forall t \in \mathcal{T} \quad (11a)$$

$$p_g^t + p_{RTO}^t + p_{CHP}^t + p_{GT}^t + p_{PV}^t + p_{WT}^t + p_{PHSD}^t = p_{PHSC}^t + p_{Load}^t + \sum_{j=1}^{N_{BC}} p_{BC,j}^t + p_{WSHP}^t, \quad \forall t \in \mathcal{T} \quad (11b)$$

$$\sum_X h_X^t + h_{TSTD}^t = h_{TSTC}^t + h_{Load}^t, \quad \forall t \in \mathcal{T} \quad (11c)$$

D. Model Reformulation

In the above model, the parameters are $\Xi_{|I|} = [p_{BC,j}, \bar{p}_{BC,j}, \underline{p}_g, \bar{p}_g, \theta_{2,j}, \forall j \in N_{BC}]$ and $x_{|I|}^{[T]}$ are other variables except $p_{BC,|I|}^{[T]}$ and $p_g^{[T]}$. The model is reformulated into an impact form in Eq. (12).

$$\min_{p_{BC,|I|}^{[T]}, p_g^{[T]}, x_{|I|}^{[T]}} C_{Sys} \quad (12)$$

s.t. Eqs. (5a) ~ (11c)

IV. SOLUTION METHODOLOGY

A. Parameter Identification

Based on historical data set $D = [p_{BC,|I}^D, p_g^D, \kappa_{Price}^D]$, the bilevel optimization problem (3) can be converted into a single level problem via KKT conditions. Thus, the data-driven inverse optimization based FRA can be formulated as follows.

$$\min_{\Xi_{|I} \in [\Xi_{|I}, \bar{\Xi}_{|I}]} \mathcal{L} = \|p_{BC} - p_{BC,|I}^{D,|T} \|_2 + \|p_g - p_g^{D,|T} \|_2 \quad (13a)$$

$$\text{s.t.} \quad \frac{\partial \mathcal{L}}{\partial p_{BC,|I}^{[T]}} = 0, \quad \frac{\partial \mathcal{L}}{\partial p_g^{[T]}} = 0, \quad \frac{\partial \mathcal{L}}{\partial x_{|I}^{[T]}} = 0 \quad (13b)$$

$$h(p_{BC,|I}^{[T]}, p_g^{[T]}, x_{|I}^{[T]}, \Xi_{|I}) = 0, \quad (13c)$$

$$g(p_{BC,|I}^{[T]}, p_g^{[T]}, x_{|I}^{[T]}, \Xi_{|I}) \leq 0, \quad (13d)$$

$$\mu \geq 0, \mu^T \perp g(p_{BC,|I}^{[T]}, p_g^{[T]}, x_{|I}^{[T]}, \Xi_{|I}), \quad (13e)$$

$$\mathcal{L}^*(\lambda, \mu) = \mathcal{L} \quad (13f)$$

where Eqs. (13b)-(13f) are the stationarity, primal feasibility, dual feasibility, complementary slackness and strong duality conditions respectively. By solving this problem with finite number of data in D , the Ω_V can be effectively approximated.

B. Learning-based FRA algorithm

Although the nonlinear complementary slackness condition in (13e) can be handled with the Big M method, it still contains a large number of binary variables. This would lead to a heavy computation burden especially when the original CMIES dispatching problem has high-dimension variables and numerous constraints. One effective approach is to leverage the learning method to get the FRA solution. To solve the nonlinear FRA problem in Eq. (13), the LFRA algorithm is proposed to solve the following inverse optimization problem (14) with the dynamic updated data. Detailed procedures are given in Algorithm 1.

$$\min_{\Xi_{|I}^\xi} \left(\mathcal{L} + \frac{\rho}{2} \left\| \Xi_{|I}^\xi - \Xi_{|I}^{\xi-1} \right\|_2 \right), \forall \xi \quad (14a)$$

$$\text{s.t.} \quad \text{Eqs. (13b) } \sim \text{(13f)} \quad (14b)$$

Algorithm 1: Learning-based FRA Algorithm

Input : Iteration index $\xi = 1$, Penalty factor ρ ,
Tolerance value ϵ , Historical data D

- 1 *Initialize*: Solve the FRA in (13) with parameter $\Xi_{|I}^0$
- 2 **while** $\| \mathcal{L}^\xi - \mathcal{L}^{\xi-1} \|_2 \geq \epsilon$ **do**
- 3 **for** $s = \xi$ **to** $\xi + |D|$ **do**
- 4 Solve (14) to obtain $\tilde{\Xi}_{|I}^{\xi,s}$
- 5 **end**
- 6 Update the $\tilde{\Xi}_{|I}^\xi = \frac{1}{|D|} \sum_{s=\xi}^{\xi+|D|} \tilde{\Xi}_{|I}^{\xi,s}$
- 7 $\xi = \xi + 1$
- 8 **end**

Output: $\tilde{\Omega}_V(\tilde{\Xi}_{|I})$

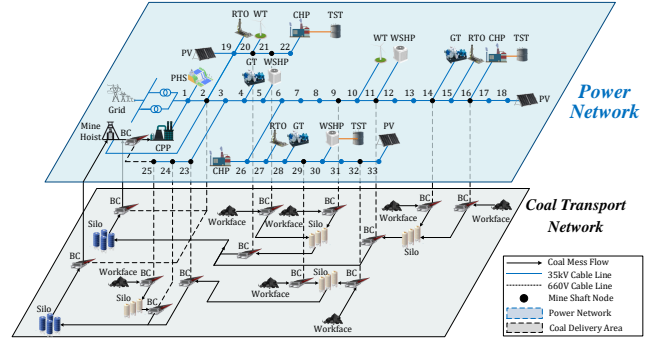


Fig. 2. System configuration

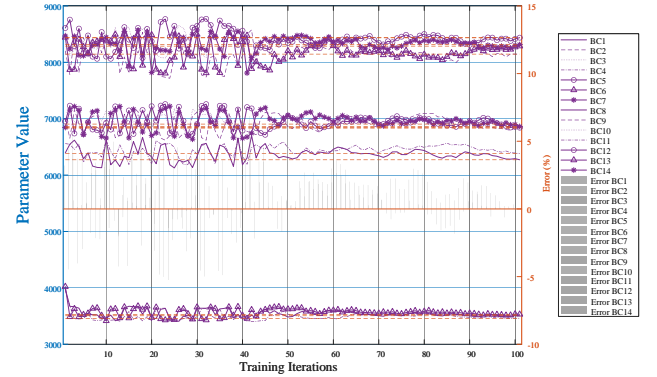


Fig. 3. The parameter identification results of 14 BCs

The LFRA algorithm iteratively optimizes parameters for high-dimensional systems. It processes scenario-specific data in a mini-batch style, updating parameters and averaging results for robustness. Convergence is achieved when the loss change meets a tolerance. This incremental learning based approach enhances adaptability and convergence efficiency.

V. CASE STUDIES

A. Test System Setup

The proposed LFRA method is numerically evaluated using the data of coal mines in IEEE 33-bus distribution system, illustrated in the Fig. 2. The FRA is solved on the MATLAB R2023b platform via Gurobi 11.0.0 using an Apple Silicon M1 CPU with 16GB RAM.

B. Parameter Identification

Fig. 3 illustrates the parameter θ_2 identification results and percentage relative errors for individual BC devices over training, revealing that the proposed LFRA can effectively approximate the unknown parameters from historical data. It is represented that there are noticeable fluctuations at the beginning of the training, which gradually reduce, indicating that the model is learning the parameters to better fit the actual ones. Near the end of training, most approximated θ_2 for diverse BCs maintain low error rates, which are under 1% and relatively acceptable in application.

TABLE I
RESULT COMPARISON ON APPROXIMATION ERROR

Method	\bar{p}_{BC}		\underline{p}_{BC}		\bar{p}_g		\underline{p}_g		θ_2	
	LSTM	LFRA	LSTM	LFRA	LSTM	LFRA	LSTM	LFRA	LSTM	LFRA
RMSE (%)	25.34	2.95	NaN	NaN	7.32	3.06	10.8	0.11	7.39	2.21
MAE (%)	25.02	5.28	NaN	NaN	7.32	5.20	10.8	0.13	7.13	1.71



Fig. 4. The FRA and error results

C. Performance Comparison

The maximum and minimum power values for BCs and power exchange within the VPP, predicted by the proposed method, are compared with true values in Fig. 4.

Results demonstrate that the proposed LFRA method effectively approximates both the maximum and minimum power bounds for belt conveyors and power exchange, validating its accuracy and reliability. The low error observed in the belt conveyor limits indicates that the method can precisely capture the stable operational characteristics of these components, likely due to the predictable nature of their power profiles. For belt conveyors power approximation, result shows an a final error below 1%, while the minimum power limit maintains an error of under 0.3% across all data points. In the case of power exchange, the approximation achieves an average error of approximately 3% for both maximum and minimum power bounds. This indicates that the proposed method can ensure the accuracy of FRA with historical data.

Table I presents a comparative analysis of approximation errors using two methods: LSTM and the proposed LFRA. The results show that the LFRA consistently outperforms LSTM across all evaluated parameters, achieving significantly lower RMSE and MAE values. Specifically, for belt conveyor maximum power, LFRA yields an RMSE of 2.95% and MAE of 5.28%, markedly lower than LSTM's RMSE and MAE values of 25.34% and 25.02%, respectively. This indicates LFRA's superior accuracy in capturing the peak-valley regulation potential of the coal mine VPP. However, due to the minimum BC power can reach 0, the RMSE and MAE for both LSTM and LFRA are NaN. Notably, when approximating \bar{p}_g and \underline{p}_g , LFRA maintains accurate approximations, while LSTM shows higher RMSE and MAE. For the parameter θ_2 , LFRA achieves 2.21% RMSE and 1.71% MAE, while LSTM has higher errors, further confirming LFRA's accuracy advantage. These results validate LFRA's effectiveness for high-accuracy FRA in the coal mine VPP.

VI. CONCLUSION

In this study, a learning-based FRA method was developed for the coal mine VPP under imperfect information. The proposed LFRA approach demonstrates superior accuracy in approximating operational limits compared to traditional methods, achieving significantly lower RMSE and MAE across key parameters. Future work will focus on extending LFRA for real-time applications and addressing nonlinear characteristics in industrial FRA.

REFERENCES

- [1] National Bureau of Statics, *Stastical year book of China*. Beijing: China statics Press, 2020. [Online]. Available: <https://www.stats.gov.cn/sj/ndsj/2024/indexch.htm>
- [2] R. Lyu, H. Guo, Y. Zheng, Y. Bai, and Q. Chen, "Lstn: a linear model of industrial production process for demand response," in *2023 IEEE PES Innovative Smart Grid Technologies Europe (ISGT EUROPE)*. IEEE, 2023, pp. 1–5.
- [3] Z. Tan, A. Yu, H. Zhong, X. Zhang, Q. Xia, and C. Kang, "Optimal virtual battery model for aggregating storage-like resources with network constraints," *CSEE Journal of Power and Energy Systems*, 2022.
- [4] H. Zhao, B. Wang, Z. Pan, H. Sun, Q. Guo, and Y. Xue, "Aggregating additional flexibility from quick-start devices for multi-energy virtual power plants," *IEEE Transactions on Sustainable Energy*, vol. 12, no. 1, pp. 646–658, 2021.
- [5] H. Huang, R. Liang, C. Lv, M. Lu, D. Gong, and S. Yin, "Two-stage robust stochastic scheduling for energy recovery in coal mine integrated energy system," *Applied Energy*, vol. 290, p. 116759, 2021.
- [6] H. Huang, Z. Li, H. B. Gooi, H. Qiu, X. Zhang, C. Lv, R. Liang, and D. Gong, "Distributionally robust energy-transportation coordination in coal mine integrated energy systems," *Applied Energy*, vol. 333, p. 120577, 2023.
- [7] J. Ma, Y. Zhang, Y. Wang, D. Gong, X. Sun, and B. Zeng, "A multitask multiobjective operation optimization method for coal mine integrated energy system," *IEEE Transactions on Industrial Informatics*, vol. 20, no. 9, pp. 11 149–11 160, 2024.
- [8] H. Huang, Z. Li, L. P. M. I. Sampath, J. Yang, H. D. Nguyen, H. B. Gooi, R. Liang, and D. Gong, "Blockchain-enabled carbon and energy trading for network-constrained coal mines with uncertainties," *IEEE Transactions on Sustainable Energy*, vol. 14, no. 3, pp. 1634–1647, 2023.
- [9] Y. Jiang, Z. Ren, and W. Li, "Committed carbon emission operation region for integrated energy systems: Concepts and analyses," *IEEE Transactions on Sustainable Energy*, vol. 15, no. 2, pp. 1194–1209, 2024.
- [10] Y. Wen, Z. Hu, S. You, and X. Duan, "Aggregate feasible region of ders: Exact formulation and approximate models," *IEEE Transactions on Smart Grid*, vol. 13, no. 6, pp. 4405–4423, 2022.
- [11] P. Pareek, A. Singh, L. P. Mohasha, I. Sampath, H. B. Gooi, and H. D. Nguyen, "Privacy-preserving feasibility assessment for p2p energy trading and storage integration," in *2022 IEEE Power & Energy Society General Meeting (PESGM)*, 2022, pp. 1–5.
- [12] T. C. Chan and N. Kaw, "Inverse optimization for the recovery of constraint parameters," *European Journal of Operational Research*, vol. 282, no. 2, pp. 415–427, 2020.
- [13] Z. Tan, Z. Yan, Q. Xia, and Y. Wang, "Data-driven inverse optimization for modeling intertemporally responsive loads," *IEEE Transactions on Smart Grid*, vol. 14, no. 5, pp. 4129–4132, 2023.
- [14] R. Lyu, H. Guo, and Q. Chen, "Approximating energy-regulation feasible region of virtual power plants: a data-driven inverse optimization approach," in *IEEE PES General Meeting*, 2024.